



Cite this: *Phys. Chem. Chem. Phys.*,
2015, 17, 16351

Anomalous doping effect in black phosphorene using first-principles calculations

Weiyang Yu,^{ab} Zhili Zhu,^a Chun-Yao Niu,^a Chong Li,^a Jun-Hyung Cho^{*ac} and Yu Jia^{*a}

Using first-principles density functional theory calculations, we investigate the geometries, electronic structures, and thermodynamic stabilities of substitutionally doped phosphorene sheets with group III, IV, V, and VI elements. We find that the electronic properties of phosphorene are drastically modified by the number of valence electrons in dopant atoms. The dopants with an even number of valence electrons enable the doped phosphorenes to have a metallic feature, while the dopants with an odd number of valence electrons retain a semiconducting feature. This even–odd oscillating behavior is attributed to the peculiar bonding characteristics of phosphorene and the strong hybridization of sp orbitals between dopants and phosphorene. Furthermore, the calculated formation energies of various substitutional dopants in phosphorene show that such doped systems can be thermodynamically stable. These results propose an intriguing route to tune the transport properties of electronic and photoelectronic devices based on phosphorene.

Received 25th March 2015,
Accepted 18th May 2015

DOI: 10.1039/c5cp01732g

www.rsc.org/pccp

1. Introduction

The discovery of graphene has opened many new areas of research related to two-dimensional (2D) atomic-layer systems such as transition metal dichalcogenides (TMDCs), silicene, germanane, and so on.^{1–4} All of them have attracted much attention as promising materials for future electronics applications.^{5,6} Most recently, few-layer black phosphorus (BP) was successfully fabricated through exfoliation techniques,⁷ and especially monolayer BP (termed phosphorene) becomes another stable elemental 2D material. Because of its intriguing electronic properties, phosphorene has drawn much attention in both experimental and theoretical studies.^{8–15} Interestingly, few-layer BP has been theoretically predicted to have a direct gap or a nearly direct gap ranging from 0.8 to 2 eV depending on the layer thickness.⁸ It was reported that phosphorene has a high carrier mobility of $\sim 10^3 \text{ cm}^2 \text{ V}^{-1} \text{ s}^{-1}$ and an on/off ratio of $\sim 10^4$ at room temperature, thus it is considered as a novel channel material in field effect transistors. Recently, Shao *et al.*¹⁶ predicted that phosphorene could become a potential superconductor material through electron-doping, and Jing *et al.*¹⁷ investigated the optical properties of phosphorene by molecular

doping. These exotic electronic properties of phosphorene can be utilized for the development of future nanoelectronic devices.^{18–20}

Doping in 2D materials is of fundamental importance to enable a wide range of optoelectronic and electronic devices by tuning their electronic properties. For graphene, it has been well established that carrier concentration can be modulated by charge-transfer doping with adsorbed atoms, molecules, and clusters.^{21–25} Here, the Fermi level can be shifted above or below the Dirac point depending on n or p doping, respectively.²⁶ Alternatively, substitutional doping in graphene with heteroatoms provides an effective route for simple and stable tuning of doping levels. Although the electronic properties of pure phosphorene have been extensively studied,^{16–19,21} there are, to the best of our knowledge, few theoretical and experimental investigations into the effect of various dopants on the electronic properties of phosphorene.

In this work, we perform a systematic study of the substitutional doping of phosphorene with group III, IV, V, and VI elements, respectively. Based on first-principles density functional theory (DFT) calculations, we demonstrate that the electronic properties of phosphorene can be tuned depending on the number of valence electrons in dopant atoms: *i.e.*, group IV and VI elements with an even number of valence electrons induce a metallic feature, while group III and V elements with an odd number of valence electrons preserve the semiconducting feature of pure phosphorene. The underlying physics of such an even–odd oscillation effect in doped phosphorenes can be explained by the sp³ bonding character of P atoms with a lone pair of valence electrons and their strong hybridizations with the sp orbitals of dopants.

^a International Laboratory for Quantum Functional Materials of Henan, and School of Physics and Engineering, Zhengzhou University, Zhengzhou, 450001, China. E-mail: jiayu@zzu.edu.cn; Tel: +86-371-6773-9336

^b School of Physics and Chemistry, Henan Polytechnic University, Jiaozuo 454000, China

^c Department of Physics and Research Institute for Natural Sciences, Hanyang University, 17 Haengdang-Dong, Seongdong-Ku, Seoul 133-791, Korea. E-mail: chojh@hanyang.ac.kr

Additionally, the thermodynamic stabilities of substitutionally doped phosphorene are also studied by the analysis of formation energy, showing that the doping systems can be realized experimentally.

2. Computational method

Our DFT calculations within the general gradient approximations (GGA) have been performed using the Vienna *ab initio* simulation package (VASP) code.²⁷ We used the Perdew–Burke–Ernzerhof (PBE)²⁸ exchange–correlation functional for the GGA. The projector augmented wave (PAW) method²⁹ was employed to describe the electron–ion interaction. In the structural optimization, all the atoms in the modeling systems were allowed to relax until all the residual force components were less than $0.01 \text{ eV } \text{Å}^{-1}$. For the calculations of the density of state (DOS), the tetrahedron method is used with a quick projection scheme. For the calculations of the band structures, we use Gaussian smearing in combination with a small width of 0.05 eV , and the path of integration in the first Brillouin zone is along $\Gamma(0.0, 0.0, 0.0) \rightarrow \Gamma(0.0, 0.0, 0.0) \rightarrow X(0.5, 0.0, 0.0) \rightarrow M(0.5, 0.5, 0.0)$. A kinetic energy cutoff of 500 eV was used in all calculations.

The present substitutionally doped phosphorene systems were modeled in periodic slab geometry, where a series of 2×2 and 4×4 supercells of the phosphorene sheet was used with a vacuum spacing of $\sim 15 \text{ Å}$ between adjacent phosphorene sheets, respectively. Here, one P atom in 2×2 or 4×4 supercells was substituted by a dopant atom, as shown in Fig. 1(a) and (b), leading to a doping concentration of 6.25% and 1.56%, respectively. The k -space integration was done with $8 \times 10 \times 1$ and $4 \times 4 \times 1$ k points in the 2×2 and 4×4 surface Brillouin zone, respectively, generated by the Monkhorst–Pack scheme.³⁰ To test our results, we have used relatively large supercells up to 5×5 and 6×6 for all the dopants with smaller concentration of 1.00% and 0.69%, respectively, and we obtained

the same trend. Therefore, we present here our results of 2×2 or 4×4 supercells. Finally, for the $4 \times 4 \times 2$ supercell for bulk doping calculation and 4×8 supercell for two element codoping, the k points of $3 \times 3 \times 3$ and $2 \times 2 \times 1$ were applied, respectively. The distance of two dopants in the codoping systems is set to 4.33 Å in order to model the random distribution of dopants.

3. Results and discussion

To obtain the stable geometric structures of the doped systems, we optimize the atomic structure of each substitutionally doped phosphorene. The calculated geometric parameters are listed in Table 1, and the bond lengths, denoted as d_1 and d_2 , and bond angles, θ_1 and θ_2 , in Fig. 1(a) and (b), respectively. The dopants we study here are B, C, N, O, Al, Si, S, Ga, Ge, As and Se from group III to group VI. The geometric parameters of pure phosphorene are also listed for comparison. From our DFT calculations, these geometric parameters of pure phosphorene agree well with those obtained using a previous calculation³¹ (see Table 1). In the doped phosphorene, we find that the d_1 and d_2 (θ_1 and θ_2) values of B, C, N, and O dopants are smaller than the corresponding ones of pure phosphorene, because of the much smaller atomic radii of B, C, N and O atoms compared with the P atom. While the geometric parameters in Al, Si and S doped phosphorenes are close to those of pure phosphorene because they are in the same period as the P atom in Periodic Table of Elements, the structural parameters in Ga, Ge, As and Se doped phosphorenes are larger than that of pure phosphorene on account of the larger atomic radii.

Now, we begin to investigate the electronic structures of the doped phosphorene. We first chose a 2×2 supercell in which one P atom was replaced by a dopant to simulate the larger doping concentration of 6.25%. The calculated band structures of B, C, N, O, Al, Si, S, Ga, Ge, As and Se doped phosphorenes, together with that of pure phosphorene, are plotted in Fig. 2. From the band structure of pure phosphorene, we find that the valence band is occupied while the conduction band is unoccupied with a band gap of about 1 eV in our calculation, which is in

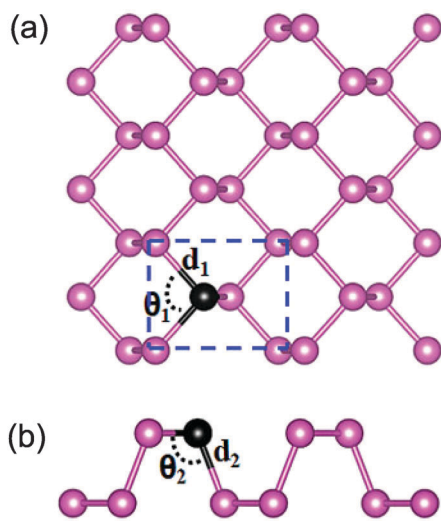


Fig. 1 The schematic of phosphorene, (a) top view and (b) side view. The P atom substituted by a dopant atom is drawn with a dark circle. The bond lengths (d_1 and d_2) and bond angles (θ_1 and θ_2) are represented in Table 1.

Table 1 Calculated bond lengths (d_1 and d_2) and bond angles (θ_1 and θ_2) of the 2×2 supercell of B, C, N, O, Al, Si, S, Ga, Ge, As and Se doped phosphorenes, respectively, together with those of pure phosphorene. For comparison, previous theoretical results for pure phosphorene are also given

Dopant atom	d_1 (Å)	d_2 (Å)	θ_1 (°)	θ_2 (°)
Pure	2.24	2.26	96.6	101.6
Pure ³¹	2.25	2.26	96.9	102.3
B	1.95	1.88	108.7	122.3
C	1.81	1.80	107.2	120.6
N	1.80	1.80	104.9	119.0
O	2.11	1.75	110.4	117.1
Al	2.36	2.35	97.3	118.2
Si	2.27	2.30	96.0	106.8
S	2.18	2.97	99.1	103.3
Ga	2.36	2.35	100.5	119.8
Ge	2.26	2.26	96.2	103.9
As	2.35	2.39	93.9	104.3
Se	2.32	3.02	99.1	94.6

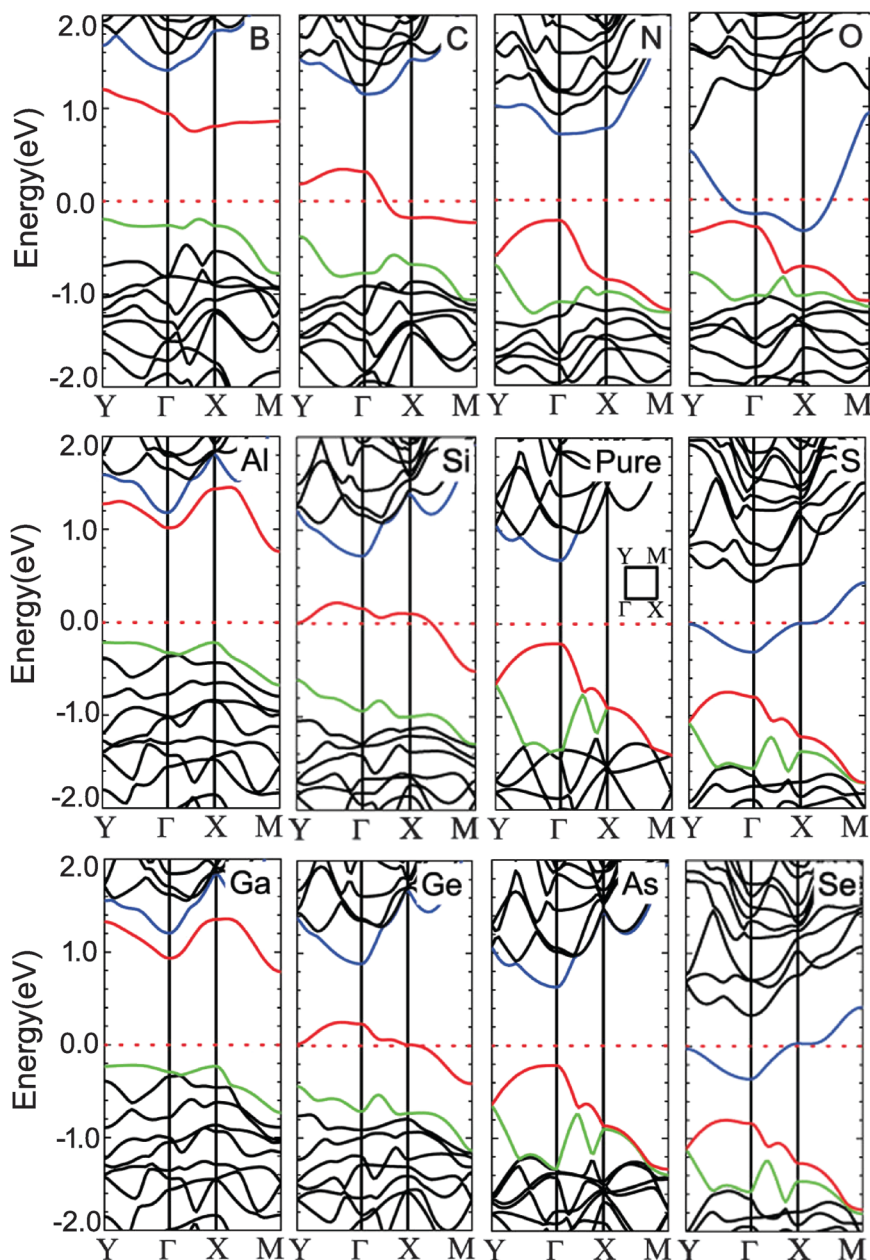


Fig. 2 Calculated band structures of the 2×2 supercell with various dopants in phosphorenes from group III, IV, V, and VI, respectively, together with that of pure phosphorene. The band dispersions are plotted along the symmetry lines shown in the surface Brillouin zone (see the inset). The energy zero represents the Fermi level.

agreement with other previous calculations.³¹ For the doped systems, we can see that the Fermi levels in C, Si, Ge and B, Al, Ga doped phosphorenes shift downward toward the valence band while that in O, S, Se doped phosphorenes shift upward toward the conduction band, as shown in Fig. 2. More interestingly, the electronic properties of doped phosphorene systems are determined dramatically by the number of valence electrons in dopant atoms: *i.e.*, C, Si, Ge and O, S, Se atoms with an even number of valence electrons give rise to metallic features while doping atoms with an odd number of valence electrons (such as B, Al, Ga and N, As) remain semiconducting.

To investigate whether the above metallic–semiconducting oscillation with a number of the valence electrons is general, we calculate the band structures of various dopants using a relatively large 4×4 supercell with a smaller concentration of 1.56%. The results are shown in Fig. 3. From Fig. 3, the even–odd oscillation behaviors can also be found as the same as in Fig. 2. Besides this, we noticed that such interesting properties are still preserved by reducing the doping concentration up to 1% or even less than this, *i.e.* some 5×5 and 6×6 supercells were used in the calculations. Of course, if the doping concentrations become very small, the even–odd oscillations will disappear undoubtedly. Therefore, in the

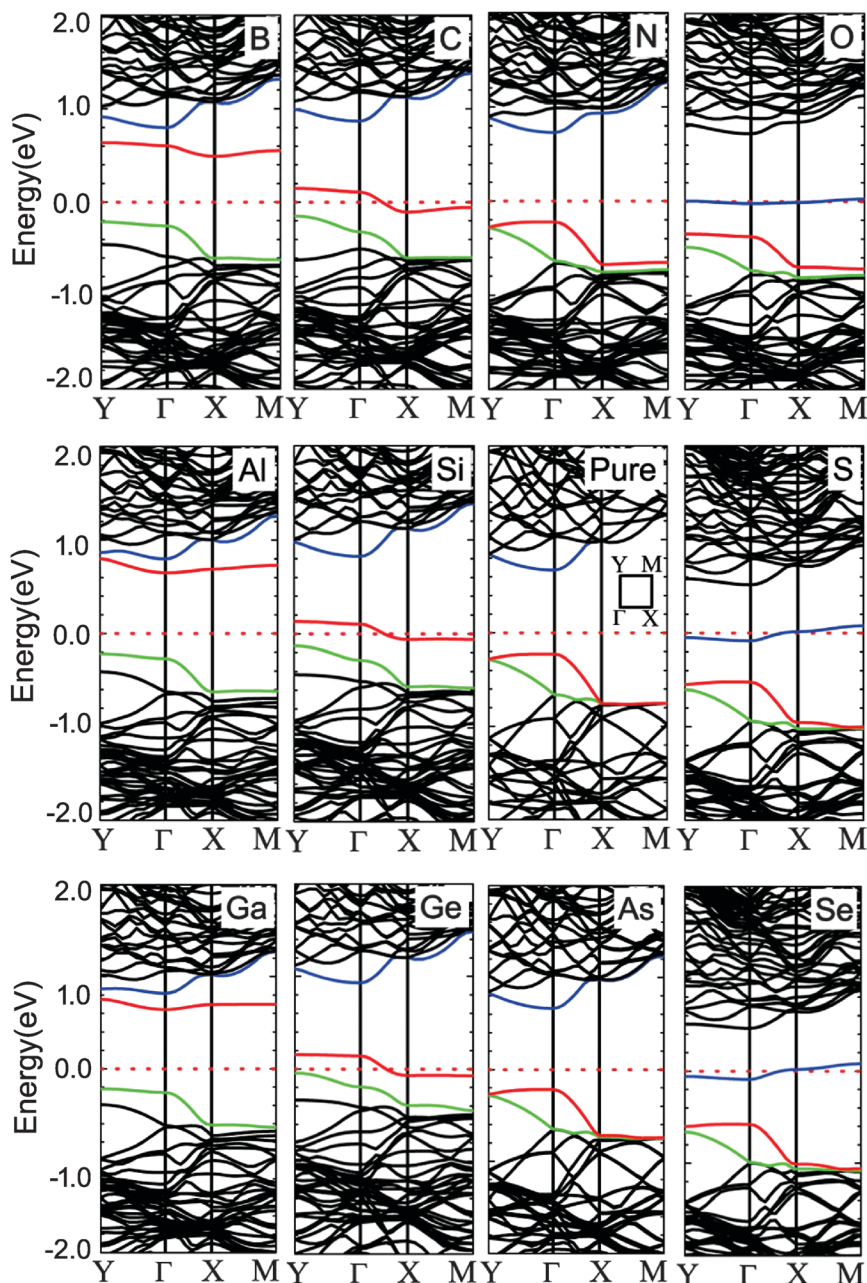


Fig. 3 Calculated band structures of the 4×4 supercell with various dopants in phosphorenes from group III, IV, V, and VI, respectively, together with that of pure phosphorene. The band dispersions are plotted along the symmetry lines shown in the surface Brillouin zone (see the inset). The energy zero represents the Fermi level.

following we will focus our discussions on a relatively high doping concentration.

We have summarized the general trend of the above-mentioned even-odd oscillation behaviors for 2×2 and 4×4 supercells in Fig. 4. The oscillating schematic diagram in Fig. 4 demonstrates the calculated band gaps (E_g) of various dopants in phosphorene. From Fig. 4 we can see that for the 4×4 supercell, the band gaps of B, Al, and Ga (N, As) doped phosphorenes are 0.84, 1.12, and 0.89 (0.95, 0.88) eV, respectively, while the band gap of pure phosphorene is 0.90 eV, which is consistent with the results of Liang *et al.*³² For the 2×2 supercell

the band gaps of B, Al, and Ga (N, As) doped phosphorenes are 1.12, 0.93, and 1.05 (0.90, 0.89) eV, which is almost the same as that of 4×4 supercells. It is seen that the band gap oscillates depending on even and odd numbers of valence electrons in dopant atoms. Here, group IV (C, Si and Ge) or group VI (O, S and Se) doped phosphorenes that have odd number of electrons per unit cell exhibit a metallic feature with a half-filled band at the Fermi level. On the other hand, group III (B, Al and Ga) or group V (N and As) doped phosphorenes containing even number of electrons per unit cell have fully occupied valence bands, showing a semiconducting feature. Generally speaking, the decrease(increase) of gap opening

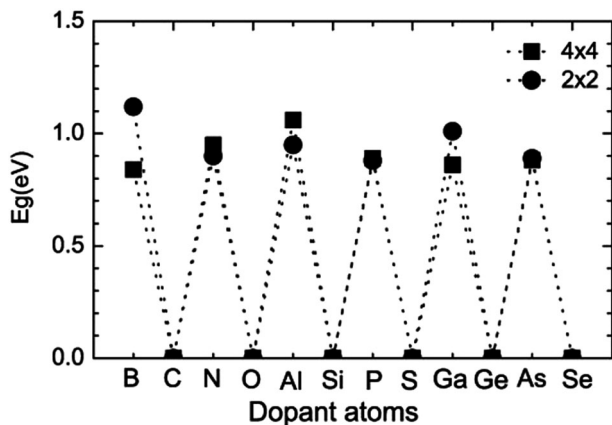


Fig. 4 Calculated band gaps of substitutionally doped phosphorenes with various dopants from group III, IV, V, and VI, respectively.

in doped phosphorenes is most likely to be associated with the strong hybridization of p orbitals between dopants and phosphorenes, as discussed below.

The presence of metallic and semiconducting properties in doped phosphorenes can be associated with the bonding nature of phosphorene where each P atom (having valence electron configuration $3s^23p^3$) forms sp^3 bonding with a lone pair of valence electrons.³³ In doped phosphorenes, the non-bonding lone-pair electronic states of pure phosphorene are easily tuned by the valence-electron states of dopant atoms, leading to the semiconducting or metallic electronic states near the Fermi level, as shown in Fig. 2 and 3. Furthermore, we have plotted the difference in charge densities between the doped system and pure phosphorene in Fig. 5 for B, C, N and O-doped systems, respectively. From Fig. 5 we can see that for N-doped phosphorene, three electrons of N are involved in the bonding between N and neighboring P atoms, leaving one lone pair of electrons on each atom, which makes the N-doped system keep the same semiconducting properties as pure phosphorene. While for B-doped phosphorene, the lone pairs on B atoms disappear because of the only three valence electrons bonding to neighboring P atoms, keeping also semiconducting properties.

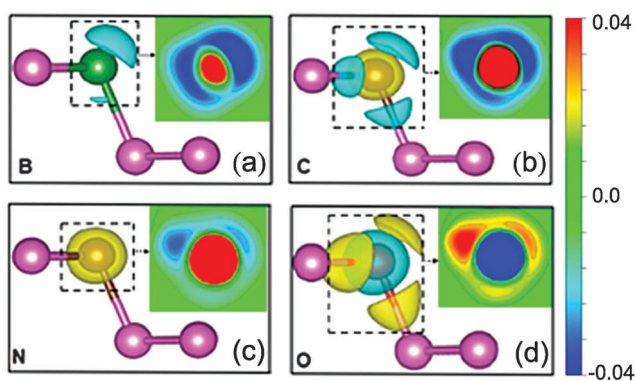


Fig. 5 Schematic diagrams of different charge densities $\Delta\rho = \rho_{\text{doped}} - \rho_{\text{pure}}$ of (a) B, (b) C, (c) N and (d) O doped phosphorenes, respectively. Iso surfaces correspond to $0.04 \text{ e}^- \text{ \AA}^{-3}$.

As for C-doped phosphorene, there is only one electron not involved in, leading to a half-filled delocalized energy band. While for O-doped phosphorene, three non-bonding electrons also give rise to the half-filled state, presenting metallic properties. Our findings of the metal–semiconductor oscillatory behaviors in doped phosphorene systems contrast with the conventional doping effect in group IV semiconductors, where n- and p-type dopants create some localized doping-induced states in the band gap.

To further shed light on the underlying bonding mechanism of the dopants and the phosphorus atoms, we show in Fig. 6 the total and partial density of states (PDOS) of B, C, N and O-doped phosphorenes, respectively. As shown in Fig. 6, the calculated partial density of states (DOS) projected onto the 2p orbitals of each dopant atom shows similar pattern and peak positions to that for the P atom, indicating a strong hybridization of sp orbitals between dopants and phosphorene. This strong hybridization leads to a broadening of the partial DOS for dopants. Especially, for C(O) doped phosphorene, the 2p partial DOS peaks for the C(O) dopant and P atom locate at the Fermi level, thereby giving rise to a metallic property. We have double-checked the results using spin-polarized calculations especially for the metallic behavior of dopants with an even number of valence electrons. The spin-polarized calculations show that there is no spin split at the Fermi level. So, the results of the metallic properties for dopants with an even number of valence electrons are accurate.

On the other hand, compared with the electronic properties of the monolayer doped phosphorene, the odd–even oscillation behavior in doped bulk black phosphorus does not exist

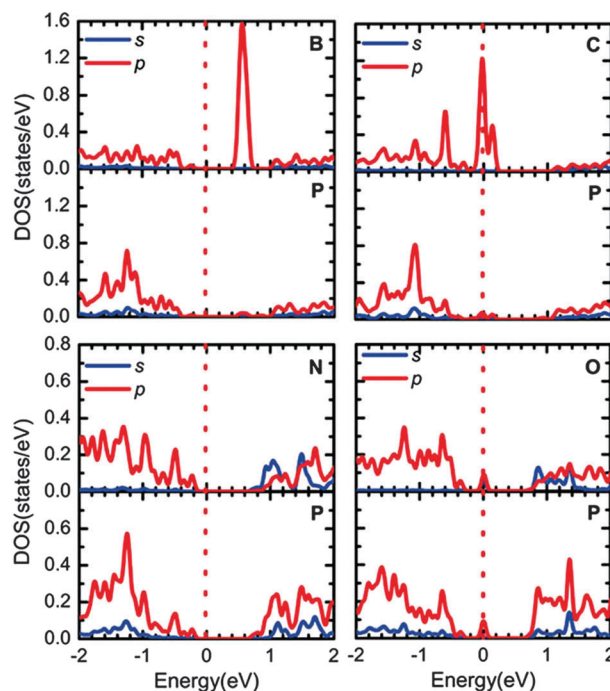


Fig. 6 Partial DOS of B, C, N and O doped phosphorenes. The partial DOS projected onto the 2s and 2p orbitals of the dopant and its bonding P atom are displayed. The energy zero represents the Fermi level.

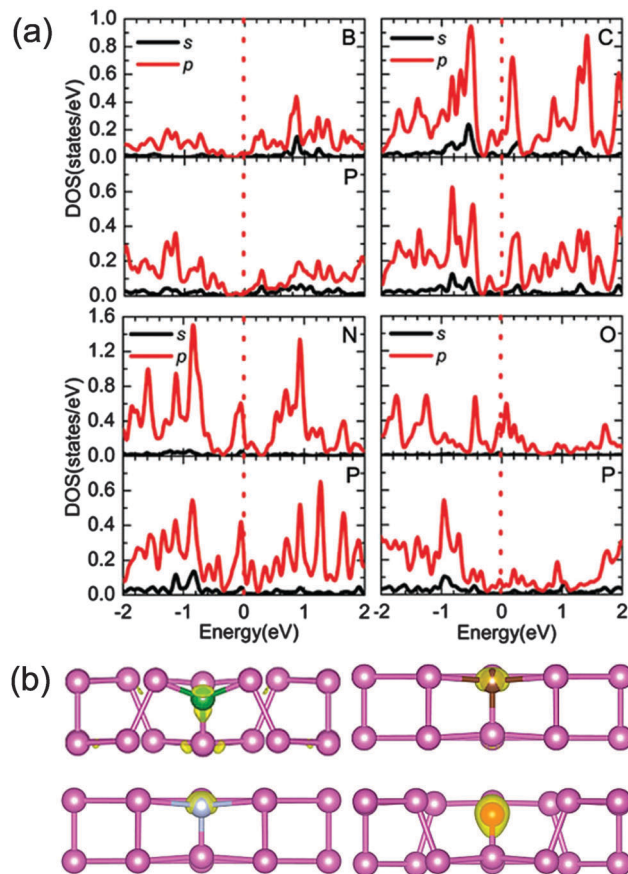


Fig. 7 (a) Density of states of substitutional B, C, N, and O doped bulk black phosphorus. Energies refer to the Fermi energy. (b) Side view of band decomposed charge density of bulk black phosphorus with energy from -1 to 1 eV around the Fermi level. Iso surfaces correspond to $0.02 \text{ e } \text{Å}^{-3}$.

any more. The reason is that, owing to the van der Waals interaction between the interlayers in bulk black phosphorus, there is no lone pair of electrons on the atoms of either the pure or doped black phosphorus. This point can simply be illustrated from the DOS of the doped bulk black phosphorus. In Fig. 7(a), we plot the DOS of B-, C-, N-, and O-doped bulk black phosphorus with a concentration of 0.39% for $4 \times 4 \times 2$ supercell simulations. From Fig. 7(a) we can see that the peaks of DOS exit at the Fermi level, both in the B(N)-doped systems and in the C(O)-doped systems. This suggests that there may be impurity states in the doping systems. Indeed, the impurity states originate from the dopant atoms, as shown in Fig. 7(b). In all, it is different from the two dimensional doping systems because of the low dimensional size effect, as mentioned above.

Our above new findings provide a new approach to tune the electronic properties by dopants with two types of different elements and different number of valence electrons. For example, we can tune the 2D phosphorene by doping with two different dopant atoms, namely co-doping.³⁴ We perform a 4×8 supercell calculation in which two P atoms were replaced by two different elements, such as B and N, B and C, and C and O, respectively. The co-doped phosphorene systems exhibit nontrivial behavior, the calculation results are shown in Fig. 8. The band structure

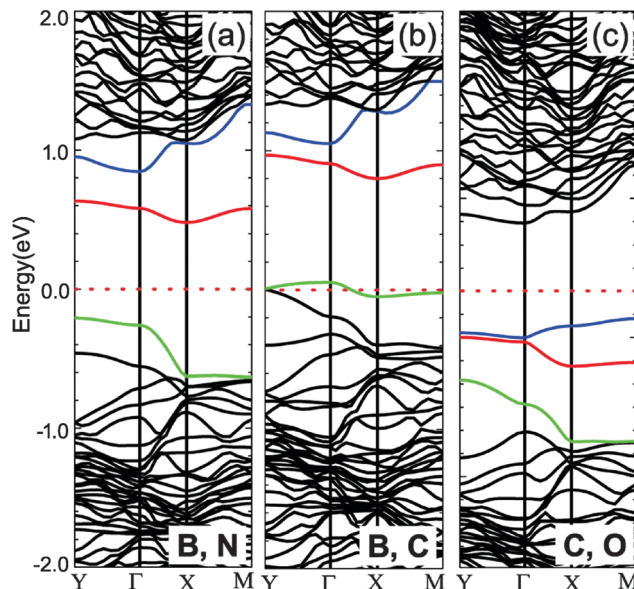


Fig. 8 Calculated band structures of (a) B and N codoped phosphorene, (b) B and C codoped phosphorene, and (c) C and O codoped phosphorene, respectively. The energy zero represents the Fermi level.

of B and N co-doped phosphorene is shown in Fig. 8(a). It is natural that the B and N co-doped system displays a semiconducting property. As for B and C co-doped phosphorene, as shown in Fig. 8(b), the band structure exhibits metallic properties because of the odd and even valence electrons. However, for C and O co-doped phosphorene, as shown in Fig. 8(c), the band structure also exhibits a semiconducting property. It is not difficult to understand that the valence band of C and O co-doped phosphorene is fully occupied, leading to a semiconducting property.

Finally, it is reasonable to question that whether such doping system can be realized experimentally. To meet this query, we examine the thermodynamic stability of doped phosphorene by

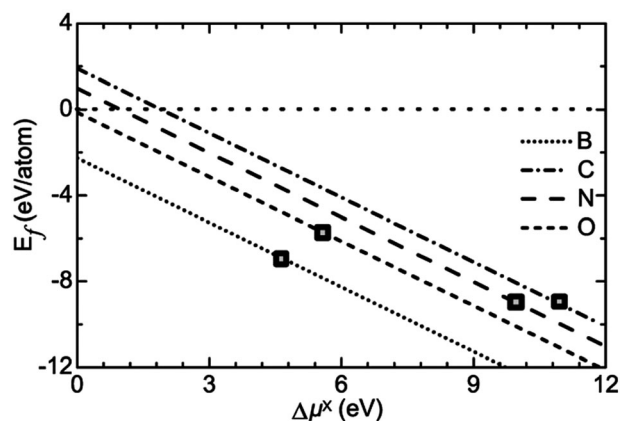


Fig. 9 Calculated formation energies of substitutional B, C, N and O doping in phosphorene as a function of the chemical potential difference of each dopant atom. The reference zero of $\Delta\mu^X$ represents the chemical potential obtained from orthorhombic B bulk, graphite, N_2 and O_2 , respectively. The formation energies estimated from the atomic chemical potential of each dopant are marked with squares.

calculating the formation energy of substitutional doping which is defined as $E_f = (E_{\text{tot}}^{\text{P+X}} + \mu^{\text{P}}) - (E_{\text{tot}}^{\text{P}} + \mu^{\text{X}})$. Here, $E_{\text{tot}}^{\text{P+X}}$ and $E_{\text{tot}}^{\text{P}}$ denote the total energies of X-doped phosphorene and pure phosphorene, respectively; μ^{P} is the chemical potential of phosphorus (taken from pure phosphorene) while μ^{X} is the chemical potential of X dopant atom. The calculated formation energies of B, C, N, and O doped phosphorenes are plotted as a function of $\Delta\mu^{\text{X}}$ in Fig. 9. We find that, if we take μ^{X} from the energies of orthorhombic B bulk, graphite, O_2 , and N_2 , the formation energies of C and N (B and O) doped phosphorenes become positive (negative), indicating an energy cost (gain) for the substitutional doping. However, all the formation energies become negative (marked with squares in Fig. 9) by assuming μ^{X} at their respective upper limits, *i.e.*, at their atomic energies. Thus, we can say that the substitutional B and O doping can be easily realized in experiments, but the substitutional C and N ones need to be particularly cautious in the synthesis processes such as atomic deposition rate, temperature, and other experimental conditions.

4. Conclusions

In conclusion, the electronic properties of substitutionally doped phosphorenes with group III, IV, V, and VI elements have been systematically investigated using first-principles DFT calculations. We found that group IV and VI dopants with an even number of valence electrons produce the metallic properties whereas group III and V dopants with an odd number of valence electrons preserve the semiconducting properties. This even-odd behavior of the electronic properties of doped phosphorenes is revealed to be due to the strong hybridization of sp orbitals between dopants and phosphorenes. The estimated formation energies of the substitutional B, C, N, and O doped phosphorenes provide information about their thermodynamic stabilities, which can be realized in experiments. Our new findings of substitutionally doped phosphorenes are drastically different from those of the conventional n- or p-type doping effect in group IV semiconductors. The novel metal–semiconductor oscillations predicted here not only provide an intriguing route to tune the transport properties of electronic devices based on phosphorene materials, but also stimulate experimentalists to develop new phosphorene-based nanoelectronic devices.

Acknowledgements

We thank Prof Zhenyu Zhang for helpful discussions. This work was supported by the National Basic Research Program of China (Grant No. 2012CB921300), the National Natural Science Foundation of China (Grant No. 11274280 and 11304288), and the National Research Foundation of Korea (Grant No. 2014M2B2A9032247).

References

1 A. K. Geim and I. V. Grigorieva, Van der Waals heterostructures, *Nature*, 2013, **499**, 419.

2 Q. H. Wang, K. Kalantar-Zadeh, A. Kis, J. N. Coleman and M. S. Strano, Low frequency electronic Noise in single-layer MoS_2 transistors, *Nat. Nanotechnol.*, 2012, **7**, 699.

3 P. Vogt, P. D. Padova, C. Quaresima, J. Avila, E. Frantzeskakis, M. C. Asensio, A. Resta, B. Ealet and G. L. Lay, Silicene: compelling experimental evidence for graphenelike two-dimensional silicon, *Phys. Rev. Lett.*, 2012, **108**, 155501.

4 E. Bianco, S. Butler, S. Jiang, O. D. Restrepo, W. Windl and J. E. Goldberger, Stability and exfoliation of germanane: a germanium graphane analogue, *ACS Nano*, 2013, **7**, 4414.

5 S. Z. Butler, S. M. Hollen, L. Cao, Y. Cui and J. A. Gupta, *et al.* Progress, Challenges, and Opportunities in Two-Dimensional Materials Beyond Graphene, *ACS Nano*, 2013, **7**, 2898.

6 S. Zhang, C. Li, S. F. Li, Q. Sun, Z. X. Guo and Y. Jia, Intrinsic spin dependent and ferromagnetic stability on edge saturated zigzag graphene-like carbon-nitride nanoribbons, *Appl. Phys. Lett.*, 2014, **104**, 172111.

7 E. S. Reich, Phosphorene excites materials scientists, *Nature*, 2014, **506**, 19.

8 V. Tran, R. Soklaski, Y. F. Liang and L. Yang, Layer-controlled band gap and anisotropic excitons in few-layer black phosphorus, *Phys. Rev. B: Condens. Matter Mater. Phys.*, 2014, **89**, 235319.

9 R. X. Fei and L. Yang, Strain-engineering the anisotropic electrical conductance of few-Layer black phosphorus, *Nano Lett.*, 2014, **14**, 2884.

10 R. X. Fei and L. Yang, Lattice vibrational modes and Raman scattering spectra of strained phosphorene, *Appl. Phys. Lett.*, 2014, **105**, 083120.

11 V. Tran and L. Yang, Unusual Scaling Laws of the Band Gap and Optical Absorption of Phosphorene Nanoribbons, *Phys. Rev. B: Condens. Matter Mater. Phys.*, 2014, **89**, 245407.

12 Z. L. Zhu, C. Li, W. Y. Yu, D. H. Chang, Q. Sun and Y. Jia, Magnetism of zigzag edge phosphorene nanoribbons, *Appl. Phys. Lett.*, 2014, **105**, 113105.

13 T. Hu, Y. Han and J. M. Dong, Mechanical and electronic properties of monolayer and bilayer phosphorene under uniaxial and isotropic strains, *Nanotechnology*, 2014, **25**, 455703.

14 T. Hu and J. M. Dong, Geometric and electronic structures of mono- and di-vacancies in phosphorene, *Nanotechnology*, 2015, **26**, 065705.

15 A. Manjanath, A. Samanta, T. Pandey and A. K. Singh, Semiconductor to metal transition in bilayer phosphorene under normal compressive strain, *Nanotechnology*, 2015, **26**, 075701.

16 D. F. Shao, W. J. Lu, H. Y. Lv and Y. P. Sun, Electron-doped phosphorene: a potential monolayer superconductor, *Europhys. Lett.*, 2014, **108**, 67004.

17 Y. Jing, Q. Tang, P. He, Z. Zhou and P. W. Shen, Small molecules make big differences: molecular doping effects on electronic and optical properties of phosphorene, *Nanotechnology*, 2015, **26**, 095201.

18 M. Buscema, D. J. Groenendijk, S. I. Blanter, G. A. Steele, H. S. J. van der Zant and A. C. Gomez, Fast and broadband photoresponse of few-Layer black phosphorus field-Effect transistors, *Nano Lett.*, 2014, **14**, 3347.

- 19 L. Li, Y. Yu, G. J. Ye, Q. Ge, X. Ou, H. Wu, D. Feng, X. H. Chen and Y. B. Zhang, Black phosphorus field-effect transistors, *Nat. Nanotechnol.*, 2014, **9**, 372.
- 20 X. Ling, H. Wang, S. Huang, F. Xia and M. S. Dresselhaus, The renaissance of black phosphorus, *Proc. Natl. Acad. Sci. U. S. A.*, 2015, **15**, 4523.
- 21 S. Y. Shin, N. D. Kim, J. G. Kim, D. Y. Noh and K. S. Kim, Control of the plasmon in a single layer graphene by charge doping, *Appl. Phys. Lett.*, 2011, **99**, 082110.
- 22 S. Thongrattanasiri, I. Silveiro and F. J. Garcia de Abajo, Plasmons in electrostatically doped graphene, *Appl. Phys. Lett.*, 2012, **100**, 201105.
- 23 R. M. Guzmán-Arellano, A. D. Hernández-Nieves, C. A. Balseiro and G. Usaj, Diffusion of fluorine adatoms on doped graphene, *Appl. Phys. Lett.*, 2014, **105**, 121606.
- 24 L. F. Huang, M. Y. Ni, G. R. Zhang, W. H. Zhou, Y. G. Li, X. H. Zheng and Z. Zeng, Modulation of the thermodynamic, kinetic, and magnetic properties of the hydrogen monomer on graphene by charge doping, *J. Chem. Phys.*, 2011, **135**, 064705.
- 25 Z. Zhang, H. Huang, X. Yang and L. Zang, Tailoring electronic properties of graphene by C stacking with aromatic molecules, *J. Phys. Chem. Lett.*, 2011, **2**, 2897.
- 26 L. Tsetseris, B. Wang and S. T. Pantelides, Substitutional doping of graphene: the role of carbon divacancies, *Phys. Rev. B: Condens. Matter Mater. Phys.*, 2014, **89**, 035411.
- 27 G. Kresse and J. Furthmüller, Efficient iterative schemes for *ab initio* total-energy calculations using a plane-wave basis set, *Phys. Rev. B: Condens. Matter Mater. Phys.*, 1996, **54**, 11169.
- 28 J. P. Perdew, K. Burke and M. Ernzerhof, Generalized gradient approximation made simple, *Phys. Rev. Lett.*, 1997, **78**, 1396.
- 29 G. Kresse and D. Joubert, From ultrasoft pseudopotentials to the projector augmented-wave method, *Phys. Rev. B: Condens. Matter Mater. Phys.*, 1999, **59**, 1758.
- 30 H. J. Monkhorst and J. D. Pack, Special points for Brillouin-zone integrations, *Phys. Rev. B: Solid State*, 1976, **13**, 5188.
- 31 Y. L. Du, C. Y. Ouyang, S. Q. Shi and M. S. Lei, *Ab initio* studies on atomic and electronic structures of black phosphorus, *J. Appl. Phys.*, 2010, **107**, 093718.
- 32 L. Liang, J. Wang, W. Lin, B. G. Sumpter, V. Meunier and M. Pan, Electronic bandgap and edge reconstruction in phosphorene materials, *Nano Lett.*, 2014, **14**, 6400.
- 33 A. N. Rudenko and M. I. Katsnelson, Quasiparticle band structure and tight-binding model for single- and bilayer black phosphorus, *Phys. Rev. B: Condens. Matter Mater. Phys.*, 2014, **89**, 201408.
- 34 Z. L. Zhu, W. Y. Yu, X. Y. Ren, Q. Sun and Y. Jia, Grain boundary in phosphorene and its unique roles on C and O doping, *Europhys. Lett.*, 2015, **109**, 47003.